A simple genetic architecture and low constraint allows rapid floral evolution in a diverse and recently radiating plant genus

Jamie L. Kostyun[1,2*], Matthew J.S. Gibson[1], Christian M. King[1,3], and Leonie C. Moyle[1]

[1] Department of Biology, Indiana University, Bloomington, IN 47405

[2] Department of Plant Biology, The University of Vermont, Burlington, VT 05405

[3] Department of Evolution, Ecology and Organismal Biology, The Ohio State University, Columbus, OH 43210

* Corresponding author: Jamie.Kostyun@uvm.edu, Tel: 802-656-7670

Word count: Summary (199), Introduction (1190), Materials and Methods (1638), Results (1387), Discussion (2014), Acknowledgements (94), Total Main Text (6229), Figures (4, all in color), Tables (2), Supplementary Documents (8 Figures, 8 Tables).

Summary

- Genetic correlations among different components of phenotypes, especially resulting from pleiotropy, can constrain or facilitate trait evolution. These factors could especially influence the evolution of traits that are functionally integrated, such as those comprising the flower. Indeed, pleiotropy is proposed as a main driver of repeated convergent trait transitions, including the evolution of phenotypically-similar pollinator syndromes.
- We assessed the role of pleiotropy in the differentiation of floral and other reproductive traits between two species—*Jaltomata sinuosa* and *J. umbellata* (Solanaceae)—that have divergent suites of floral traits consistent with bee- and hummingbird-pollination, respectively. To do so, we generated a hybrid population and examined the genetic architecture (trait segregation and QTL distribution) underlying 25 floral and fertility traits.
- We found that most floral traits had a relatively simple genetic basis (few, predominantly additive, QTL of moderate to large effect), as well as little evidence of antagonistic pleiotropy (few trait correlations and QTL co-localization, particularly between traits of different classes). However, we did detect a potential case of adaptive pleiotropy among floral size and nectar traits.
- These mechanisms may have facilitated the rapid floral trait evolution observed within *Jaltomata*, and may be a common component of rapid phenotypic change more broadly.

Key Words: floral evolution, genetic co-variation, *Jaltomata*, pleiotropy, Solanaceae, QTL co-localization, QTL mapping

Introduction

One feature of phenotypic evolution is the broad variation in observed rates of trait change, both among traits within a single lineage and among lineages. How quickly phenotypes evolve and in what direction, depends not only on their genetic basis--both the number and effect size of causal loci--and the intensity and nature of selection acting upon them, but also on their associations with other traits. Because of genetic covariance, developmental and phylogenetic constraints, and/or correlated selection pressures (Agrawal & Stinchombe, 2009), phenotypic traits often do not evolve independently from one another. Among these causal mechanisms, strong genetic covariance arises either because different traits have a shared genetic basis (pleiotropy) or because they are based on genes that are physically adjacent and therefore often co-inherited (via linkage). Strong pleiotropy is often proposed to constrain phenotypic evolution by preventing correlated traits from moving efficiently towards their own (different) fitness optima (antagonistic pleiotropy). However, such shared genetic control may also promote phenotypic change if covariation is aligned in the direction of selection (adaptive pleiotropy) (Agrawal & Stinchombe, 2009; Wagner & Zhang, 2011; Smith, 2016). Nonetheless, despite some detailed studies (e.g. Ettensohn, 2013; Shrestha *et al*., 2014; Manceau *et al*., 2011; Xu & Schluter, 2015), the genetic architecture of many ecologically important traits remains unclear, including the prevalence of strong genetic associations that could shape the course of phenotypic evolution.

How shared architecture influences phenotypic change is especially relevant for suites of traits that are functionally integrated (Armbruster *et al*., 2014) -- such as the angiosperm flower (Armbruster *et al*., 2009) -- because the magnitude and direction of

pleiotropy will directly shape if and how these co-varying traits respond to selection. Further, because pleiotropy can constrain or favor particular developmental trajectories, it is often proposed to be a main driver of convergent transitions of integrated traits in different lineages (Preston *et al*., 2011; Smith, 2016). The flower is an especially promising model for assessing the role of pleiotropy in shaping phenotypic evolution. Because flowers mediate fitness through their critical reproductive role, their constituent traits (i.e. reproductive structures, perianth, and other attraction/reward features) are often highly functionally integrated (Conner, 2002; Armbruster *et al*., 2009). Moreover, repeated transitions of phenotypically similar or convergent suites of floral traits have been identified both within and across groups (Fenster *et al*., 2004; Goodwillie *et al*., 2010; Wessinger *et al*., 2016). For example, multiple parallel shifts from bee-pollination to hummingbird-pollination are associated with parallel transitions to flowers with red petals, large amounts of dilute nectar, and narrow corolla tubes within *Penstemon* (Wessinger *et al*., 2016); similarly, the evolution of the 'selfing syndrome' (i.e. reduced overall size, herkogamy, and floral rewards) often accompanies transitions from outcrossing to predominantly selfing mating systems, and has been documented in multiple lineages (Stebbins, 1974; Goodwillie *et al*., 2010). Such patterns provide an opportunity to assess the relative frequency of adaptive vs. antagonistic pleiotropy in shaping these repeated trait combinations, within a comparative phylogenetic context.

In addition to these ecological and evolutionary features, the known genetic and molecular bases of floral development (Rijpkema *et al*., 2006; Smaczniak *et al*., 2012) themselves suggest that pleiotropy might be a key component shaping floral phenotypic change, as well as provide a functionally-informed framework for identifying how

94 changes in these mechanisms can contribute to the diversification of floral traits. Under
95 the ABC(DE) model of floral development, the combinatorial action of different gene
96 products -- primarily different MADS-box transcription factors -- control transitions to
97 flowering and the specification of floral organ identities and organ maturation, by
98 promoting or repressing different downstream targets (reviewed in O'Maoileidigh *et al*.,
99 2014; Bartlett, 2017). This combinatorial function, and the ability to regulate shared or
100 partially shared downstream targets, provides a potential mechanistic explanation for
101 strong pleiotropy among floral traits. Moreover, several key regulators of floral
102 development also function during fruit and seed production (Smaczniak *et al*., 2012;
103 O'Maoileidigh *et al*., 2014); such correlated effects on fertility traits are another potential
104 way that pleiotropy could shape floral phenotypic evolution.

105 Several empirical approaches have been taken to assess the genetic architecture
106 underlying floral trait specification and evolution, and to evaluate the strength and
107 direction of pleiotropy. Classical quantitative genetic analyses have revealed varying
108 degrees of genetic covariance among floral traits (Gottlieb, 1984; Conner *et al*., 2014),
109 while numerous QTL (quantitative trait locus) mapping studies have found that loci for at
110 least some different floral traits appear to co-localize to the same genomic region(s)
111 (reviewed in Smith, 2016). Interestingly, such studies have identified more putative cases
112 of adaptive pleiotropy (e.g. QTL affect more than one trait in the direction of parental
113 trait values) than antagonistic, suggesting that adaptive pleiotropy may be a common
114 mechanism contributing to rapid floral evolution. Because QTL generally span a genomic
115 region that contains more than one gene, such QTL co-localization is consistent with, but
116 not definitive evidence of, a role of pleiotropy in shaping floral trait co-variation (e.g. see

117 Hermann *et al*., 2013). Nonetheless, identifying strong trait correlations and/or QTL co-
118 localization represents a critical step in assessing how pervasive pleiotropy could be in
119 shaping floral trait evolution.

120 In this study, we examined phenotypic (co)variation among, and the genetic
121 architecture underlying, floral and other reproductive traits within a segregating hybrid
122 population derived from two *Jaltomata* (Solanaceae) species with divergent floral traits
123 (**Figure 1**). Despite only having diversified with the last 5 million years (Sarkinen *et al*.,
124 2013; Wu *et al*., 2018), species of *Jaltomata* are highly phenotypically diverse, including
125 extensive variation in the size, shape, and color of floral traits that is absent among their
126 close relatives within *Solanum* and *Capsicum*. Indeed, phylogenetic analyses suggest
127 numerous transitions in floral traits within the genus, including several instances of
128 convergent evolution (Miller *et al*., 2011; Wu *et al*., 2018). Importantly, many of these
129 transitions appear to involve parallel changes in several different traits within a lineage
130 (e.g. from flat corollas with small amounts of lightly colored nectar to highly fused
131 corollas with large amounts of darkly colored nectar), suggesting either a shared genetic
132 basis and/or correlated selection (perhaps pollinator-mediated selection) influences these
133 trait associations.

134 Here, we identified QTL contributing to floral and other reproductive trait
135 variation within a recombinant population to: 1) examine the genetic architecture
136 underlying reproductive trait divergence; 2) assess the role of genetic linkage and/or
137 pleiotropy (via strong trait correlations and overlapping QTL) in floral trait (co)variation;
138 and 3) assess evidence for a shared genetic basis between different classes of floral trait
139 and other reproductive (specifically fertility) traits. We found evidence for a relatively

140 simple genetic basis underlying most of the examined traits, as well as positive
141 correlations and significant QTL co-localization among traits within each of three trait
142 classes (floral morphology, floral color, and fertility). Together, these features might
143 facilitate rapid changes in these traits. In comparison, we found few associations between
144 traits from different classes, and therefore little evidence for antagonistic pleiotropy
145 among these classes, which otherwise may have constrained trajectories of floral change.
146 One striking exception was an association between flower size and nectar traits that acts
147 in the direction exhibited by multiple species in the genus, suggesting that this could
148 instead be an instance of adaptive pleiotropy.
149

150 **MATERIALS AND METHODS**

151 ***Study system:*** *Jaltomata* (Schlechtendal; Solanaceae) is the sister genus to the
152 large and economically important *Solanum* (Olmstead *et al*., 2008; Sarkinen *et al*., 2013;
153 Wu *et al*., 2019), and includes approximately 60-80 species distributed from the
154 Southwestern United States to the Andean region of South America, in addition to several
155 species endemic to the Greater Antilles and the Galapagos Islands (Miller *et al*., 2011;
156 Mione *et al*., 2015). Species are highly phenotypically diverse and live in a variety of
157 habitats (e.g. tropical rainforests, rocky foothills, and *lomas* formations).

158 Here, we focused on a closely related species pair, *J. sinuosa* and *J. umbellata*,
159 that differ in a suite of floral traits that is representative of major floral suites found in
160 other species throughout the genus (**Figure 1**; **Table S1**). *Jaltomata sinuosa* has large
161 rotate flowers with purple petals and a small amount of concentrated nectar (consistent
162 with bee pollination, Fenster *et al*., 2004; Mione *et al*., 2017), while *J. umbellata* has

small short-tubular flowers with yellowish-white petals and a large amount of dilute, but dark red, nectar that is visible through the corolla tube (Kostyun & Moyle, 2017). The tubular corollas, large volume of nectar, exerted reproductive organs, and red coloration observed in this species is consistent with hummingbird pollination (Fenster *et al*., 2004). *Jaltomata sinuosa* is distributed along the Andes in South America from Venezuela to Bolivia, while *J. umbellata* is restricted to lomas formations along the Peruvian coast. Both species are self-compatible (Kostyun & Moyle, 2017) and shrubby, but differ in leaf traits such as overall size and shape, and type of trichomes. This species pair also has several incomplete, intrinsic postzygotic reproductive barriers, including quantitatively reduced fruit set and hybrid seed viability (Kostyun & Moyle, 2017).

Generation of BC_1 population and plant cultivation: We developed a segregating hybrid population by crossing *J. sinuosa* and *J. umbellata*. Viable F1 individuals in both directions of the cross produce flowers that are phenotypically intermediate between the parental genotypes (**Figure 1**), and retain reduced but sufficient levels of fertility when back-crossed to parents (Kostyun & Moyle, 2017). Because we were especially interested in the genetic basis of red nectar and a fused corolla tube (exhibited by *J. umbellata*, present but less pronounced in F1s, but absent in *J. sinuosa*; **Figure 1; Figure S7**), we generated the mapping population by backcrossing a single *J. sinuosa* x *J. umbellata* F1 (as the ovule parent) to the original parental *J. sinuosa* individual (as the pollen parent). BC1 individuals were germinated in a growth chamber, and then moved to the Indiana University greenhouse and grown under the same conditions as the parental and F1 individuals (16 hour light cycle, watered twice daily, and fertilized weekly).

186 ***Trait measurements:*** We measured 25 floral and other reproductive traits within
187 our mapping population, F1, and parental genotypes (**Table 1; Table S2; Figure S1**).
188 Floral morphological traits were measured with hand-held calipers, and nectar volume
189 per flower was measured to the nearest 1 μL using a pipette. To reduce the potential
190 effect of daily environmental variation, nectar volume was always measured in the early
191 afternoon following watering.

192 Petal and nectar color were quantified using digital photography (Kendal *et al*.,
193 2013; Garcia *et al*., 2014): dissected whole petals or nectar drops were photographed on a
194 standard background along with white and black color standards. Light conditions were
195 standardized for all images using RAW Therapee (RAW Therapee Development Team,
196 2012), and color space attributes were measured in ImageJ (Schneider *et al*., 2012) as the
197 average value across the entire whole petal or nectar drop sample. Because RGB color
198 attributes are device-dependent (i.e. they can vary depending upon the specific camera
199 used), color values were then converted into device-independent L*a*b color attributes,
200 using the ImageJ Color Space Converter plugin (Schwartzwald, 2012). For petal and
201 nectar color, this produced three color attributes each: Lightness (L; ranges from 0
202 [black] to 100 [white]), 'a' color (more negative values correspond to more green, and
203 more positive values correspond to more magenta), and 'b' color (more negative values
204 correspond to cyan, and more positive values correspond to yellow).

205 We also measured nine fertility traits (**Table 1**) to assess the potential genetic
206 overlap between floral and other reproductive traits, as well as to examine the genetic
207 architecture underlying intrinsic postzygotic barriers between this species pair. Fruit and
208 seed related traits were measured on 2-6 crossed fruit per individual (depending on fruit

209 set). For F1 and BC1 individuals, crossed fruit were produced using pollen from the *J.*
210 *sinuosa* parental individual. To determine seed germination rates (following Farooq *et al*.,
211 2005), we soaked 10 seeds per individual in 50% bleach for 30 minutes (to soften the
212 seed coat), rinsed thoroughly, and placed on moist paper within plastic germination
213 boxes. A week after sowing, seed coats were nicked slightly and seeds were given a drop
214 of 10 mM giberellic acid (Sigma) to break dormancy. We then scored germination every
215 2 weeks for 4 months. Pollen viability was estimated from three different flowers per
216 individual, using established methods (Jewell *et al*., 2012): Briefly, for each sample all
217 undehisced anthers from a flower were collected into an eppendorf tube containing
218 aniline blue histochemical stain, gently ground with a pestle to release pollen, and viable
219 pollen grains were counted under an EVOS FL Digital Inverted Fluorescence Microscope
220 (Fisher Scientific). From these data, we also calculated the proportion of viable pollen as
221 number of viable pollen grains/total pollen grains in the sample.

222 ***Statistical analyses on phenotypic data***: Following Shapiro-Wilk tests to assess
223 normality assumptions, we transformed traits that showed a skewed distribution and/or
224 significantly non-normal residuals. In particular, we arcsine transformed proportional
225 traits (proportion of corolla fusion, fruit set, and proportion of viable pollen), and log-
226 transformed inflorescence size, corolla fusion, petal length, style length, herkogamy,
227 nectar volume, all color attributes, and remaining fertility traits. Significant differences
228 between parental species for all traits were assessed by t-tests (**Table 1**). Distribution
229 plots for all traits are provided in Supplementary Materials (**Figures S3-S6**), while
230 illustrative plots for 15 focal traits are provided in the main text (**Figure 2**). Similarly,
231 phenotypic correlations within the BC1 population were examined among all traits

232 (**Table S3**), while relationships among a subset of focal traits are presented in the main
233 text (**Figure 3**). Given significant correlations among many of the floral morphological
234 traits (**Table S3**), we also used principal component analyses (PCAs) to create separate
235 composite metrics (i.e. Morph PC1-PC3; **Table S4; Figure S2**) as additional measures of
236 floral variation. Trait correlations, including PCs, are provided in **Table S5**, and
237 distribution plots are provided in **Figure S4**.

238 ***Genotyping and linkage map construction:*** Genomic DNA was extracted from
239 young leaf tissue from the 2 parental individuals, 13 F1s (including the F1 parent used to
240 generate the population), and 269 BC1s, using the Qiagen DNeasy Plant Mini Kit. DNA
241 quantity and quality were confirmed via Nanodrop (Fisher Scientific) and gel
242 electrophoresis with λ DNA-HindIII Digest marker (New England BioLabs). Samples
243 were then sent to Novogene Corporation (Beijing) for genotyping-by-sequencing (GBS).
244 GBS libraries were prepared using optimized restriction enzymes (MseI and HaeIII), and
245 following insert size selection, sequenced on an Illumina Hi-Seq to generate 150bp paired
246 end reads. Raw reads were trimmed and filtered using Trimmomatic (Bolger *et al*., 2014),
247 and read quality was checked pre- and post-trimming using fastqc (Andrews, 2010). To
248 identify SNPs, cleaned reads were mapped to the domesticated tomato genome (Tomato
249 Genome Consortium, 2012) using the mem function in BWA (Li, 2013). Alignment files
250 were then input into the Stacks refmap pipeline (Catchen *et al*., 2013) to determine
251 genotypes. A minimum depth of six identical reads was required to create an individual
252 stack (-m parameter) and automated genotype correction was implemented during export.
253 Subsequent filtering of genotypes was performed during linkage map construction (see
254 below). Reads and genotype data are available in NCBI BioProject PRJNA514267.

255 To construct the linkage map, we first removed markers that were genotyped in
256 less than 35% of individuals, or showed significant segregation distortion (i.e. alleles at
257 >80% or <20% frequency). The linkage map was constructed using the MST and
258 Kosambi algorithms, implemented in the R package ASMap (Taylor & Butler, 2017). To
259 alleviate map expansion issues, we removed markers which consistently differed from
260 neighboring markers in terms of genotype assignment, indicating a high likelihood of
261 genotyping error. The linkage map was then finalized using the ripple function in R
262 package R/qtl (Broman *et al*., 2003).

263 ***Identifying QTL:*** We implemented Haley-Knott regression in R/qtl to identify
264 QTL contributing to each trait. To account for potential environmental contributions to
265 trait variation, we included date of measurement (Month) and location within the
266 greenhouse (Bench) as covariates in our QTL scans. Putative QTL were first identified
267 using the scanone function, followed by permutations for genome-wide LOD significance
268 thresholds. Two dimensional scans (scantwo function) were used in the stepwise qtl
269 function to fit multiple QTL models. These models were used to identify: significant
270 QTL, their 1.5 LOD confidence intervals, their effect sizes (i.e. difference in phenotype
271 mean between homozygotes and heterozygotes), the total amount of phenotypic variance
272 explained by each QTL, the proportion of parental difference explained (relative
273 homozygous effect or RHE), interactions among QTL within traits (testing evidence for
274 epistasis), and potential contributions of covariates. QTL were considered to be co-
275 localized if their 1.5 LOD intervals overlapped. Significant co-localization was assessed
276 by comparing overlap among identified QTL to overlap from 10000 randomly generated
277 distributions, for traits within each category (morphological, color/physiological, or

fertility), and between each trait category. Briefly, a custom Python script was used to generate random distributions of QTL (by randomly re-distributing the identified QTL among the 12 linkage groups), and the observed frequency of co-localization in each was recorded for each randomization to generated count distributions, in R. All code used to generate the linkage map, identify QTL, and assess QTL co-location, is available on GitHub (https://github.com/gibsonMatt/jaltomataQTL).

RESULTS

Segregation patterns suggest additive alleles underlie most floral traits

Most traits were significantly different between the two parental species (**Table 1**). F1 means were intermediate for most traits as well, except that petals were generally brighter (more white) than either parent, perhaps because F1s had lower amounts of the different pigments found in each parental species (i.e. purple pigment found in *J. sinuosa* petals, and yellow and red pigments found in *J. umbellata*) (**Figures S5+S7**). Other than fruit set and seed germination rates, all traits were unimodally distributed within the BC1s; phenotypic values were intermediate between F1s and the recurrent parent (*J. sinuosa*) for many of these traits, consistent with additive effects (**Figure 2; Figures S3-S6**). Several traits (7 of 25) showed transgressive segregation within the BC1s, including some floral morphological traits, nectar volume and color (all 3 attributes), and seed viability and germination rates (**Table S2; Figures S3-S6**).

Significant correlations observed within – but generally not between – floral morphology, floral color, and fertility trait categories

Within the BC1s, most traits were not strongly associated with one another. Nonetheless, several correlations remained significant following multiple testing (Bonferroni) correction (**Table S3**), primarily associations that are expected biologically, including allometric relationships among floral organs and positive associations among related fertility traits. For instance, corolla diameter was significantly positively associated with most other morphological traits, suggesting shared genetic control of overall floral size (**Figure 3**), while corolla diameter was also significantly negatively correlated with proportion of corolla fusion (i.e. shorter corolla tubes had wider limbs and longer tubes had narrower limbs, r = -0.348, $p = 8.68 \times 10^{-8}$). These relationships were recovered with PCA on morphology traits, in which PC1-PC3 explained 76% of the variance among BC1s (**Table S4**). Based on trait loadings, PC1 corresponds to floral width vs. depth, PC2 to overall floral size, and PC3 to relative reproductive organ dimensions. Similarly, related fertility traits also remained strongly correlated, such as fruit mass with seed set, and number of viable pollen grains with proportion of viable pollen (**Table S3**).

In contrast, there were relatively few significant correlations among different trait categories. Notable exceptions, however, included a positive relationship between corolla diameter and nectar volume, as well as several morphological traits and certain aspects of color (nectar 'b', petal 'a' and 'b') (**Figure 3; Table S3**). In particular, larger flowers tended to have more red nectar as well as more purple petals. There were also significant positive correlations between pollen viability and each of several components of flower size (as well as Morph PC2 or "size") (**Tables S3+S5**). This latter relationship seems to be explained by anther size: across 15 *Jaltomata* species, mean viable pollen count is

324 significantly associated with anther size prior to dehiscence (F = 15.56, p = 0.0017) (J.L.
325 Kostyun, unpub.).
326
327 ***Linkage map construction recovered 12 linkage groups***
328 Mapping high quality reads to the tomato genome identified 25,136 SNPs that
329 differentiated the two parental species. Following all subsequent filtering (removing
330 markers genotyped in less than 35% of individuals, with high segregation distortion or
331 non-Mendelian inheritance, or with high likelihood of genotyping errors), we retained
332 520 high quality markers. Linkage map construction recovered 12 linkage groups (LGs),
333 which correspond to the number of chromosomes in the parental species (Mione *et al*.,
334 1993; Chiarini *et al*., 2017). Total map length was 1593.71 cM (65.17 cM – 324.48 cM
335 per chromosome/LG), with an average of 2.92 cM between markers (**Figure 4**).
336
337 ***Few moderate to large-effect QTL underlie most traits, with little QTL co-localization***
338 ***between trait categories***
339 We identified QTL for 20 of our 25 examined traits, for a total of 63 QTL (with 4
340 additional loci for Morph PCs). For traits with identified QTL, most had 2-4 QTL
341 (range=1-7). Alleles at 55 of 67 QTL (82%) acted in a direction consistent with parental
342 values (i.e. the allele from paternal donor *J. umbellata* moved the phenotype of BC1s
343 closer to this species mean); at least one QTL with opposite effects was detected for 10 of
344 the 20 traits (and Morph PC1) (**Table 2**; **Table S6)**. Consistent with trait segregation
345 patterns observed in the BC1, significant interactions (epistasis) among QTL were
346 identified for only two traits: ovary diameter and nectar color 'a' (**Table 2**; **Table S6**).

347 The amount of phenotypic variation explained by each QTL ranged from 2-33%
348 (**Table 2**; **Table S6**). Of these, 19 traits (and Morph PC1 and PC3) had at least 1
349 moderate effect QTL (defined as explaining 5-25% of the variance), and 1 trait (petal
350 color 'b') had a QTL with major effect (defined as >25% variance explained) (**Table 2;**
351 **Table S6**). The lower bound of this range suggests that we had reasonable power to
352 identify QTL with even relatively small effects -- explaining as little as 2% of the
353 variance. We note however, that like most QTL analyses (Broman, 2001), we likely have
354 limited power to detect all QTL contributing to our examined traits. Nonetheless, under
355 strict additivity, QTL account for >50% of the parental difference (relative homozygous
356 effect, RHE) in 14 of the 20 traits for which we identified QTL (as well as Morph PC1-
357 3); for 8 of these traits (as well as Morph PC1-3), >75% of the parental difference is
358 accounted for (**Table 2; Table S6**). That is, for most of our traits, detected loci account
359 for the majority of parental phenotypic differences. In contrast, for four traits (corolla
360 diameter, proportion of corolla fusion, herkogamy, and inflorescence size) QTL
361 accounted for <20% of the parental difference, suggesting additional undetected loci
362 contribute to these traits. Finally, we estimated RHE >1 for 5 floral traits that also show
363 the most transgressive segregation among BC1s (nectar color 'b', petal color 'L', petal
364 length, corolla fusion, and Morph PC2) (**Table S6; Figures S3-5**).
365 Although every linkage group had at least one QTL, these were not distributed
366 uniformly across the genome, with notable clusters on LG1 and LG9 (**Figure 4; Table 2;**
367 **Tables S6+S8**). We also identified several instances of QTL co-localization within trait
368 categories, especially for morphology and fertility traits, which each had significantly
369 more cases of co-localization (1.5 LOD overlap) than expected by chance (133 observed

370 vs. upper bound of 115 expected overlaps, $p = 6.9 \times 10^{-4}$; 8 observed vs. upper bound of 4
371 expected overlaps, $p = 5.0 \times 10^{-6}$, respectively) (**Table S7; Figure S8**). These instances of
372 co-localization included QTL for biologically-related traits for which we observed strong
373 correlations, such as those underlying petal length and corolla diameter on LG8 and
374 LG12, corolla depth and corolla fusion on LG7, LG9 and LG10, and fruit mass and seed
375 set on LG11 and LG12 (**Tables S3+S8**). In some cases, co-localized QTL share the same
376 or a very close peak marker (e.g. calyx diameter and inflorescence size on LG1, and petal
377 length, corolla fusion, and ovary diameter on LG12; **Tables S6+S8**), which suggests
378 pleiotropic effects, however we note that the large 1.5 LOD intervals of some QTL will
379 increase instances of incidental co-localization events.

380 In contrast, co-localization between different trait categories was never greater
381 than expected by chance (**Table S7; Figure S8**). This is consistent with mostly incidental
382 overlap between QTL for traits in different categories. Nonetheless, we did detect co-
383 localization at the same or very close peak markers for three sets of biologically
384 interesting trait combinations: corolla diameter, proportion of corolla fusion, and petal
385 color 'L' on LG4; corolla fusion, corolla depth, and nectar color 'a' on LG7; and nectar
386 volume and nectar color 'b' on LG3 (**Figure 4; Tables S6+S8**). Not all of the traits
387 within each of these sets is significantly phenotypically correlated in the BC1 (**Table S3**),
388 especially correlations involving nectar color 'a' and 'b', possibly because these nectar
389 color traits have additional QTL that are not shared with the corolla traits or nectar
390 volume. Nonetheless, the colocalized QTL still explain large fractions of the parental
391 difference for these traits: on LG7 the QTL colocalized with corolla fusion and depth
392 explains ~20% of the parental difference in nectar color 'a', while the potentially shared

393 QTL on LG3 explains ~25% of the parental difference in nectar color 'b' and nearly 50%
394 of the parental difference in nectar volume (**Table 2; Table S6**). Together, these provide
395 intriguing cases of potential adaptive pleiotropy, such that alleles at QTL may have
396 simultaneously acted to increase corolla tube depth and nectar darkness, and increase
397 nectar production and nectar darkness, respectively.
398

399 **DISCUSSION**

400 Genetic correlations among different components of the phenotype, especially
401 resulting from pleiotropy, can constrain or facilitate trait evolution (Agrawal &
402 Stinchcombe, 2009). Pleiotropy could have particularly strong effects on the evolution of
403 traits that are functionally integrated, such as those comprising the flower (Armbruster *et*
404 *al.,* 2009; Smith, 2016). Here, we examined the genetic architecture underlying floral trait
405 evolution within florally diverse *Jaltomata*, including whether pleiotropy might have
406 shaped observed variation. We found that most of our examined traits have a relatively
407 simple genetic basis, with few to moderate QTL with largely additive effects. We also
408 identified strong correlations and significant QTL overlap within trait categories, but few
409 associations across different types of traits. The exceptions however, between certain
410 aspects of floral morphology and nectar traits (volume, and both 'a' and 'b' color), are
411 consistent with existing trait associations that are observed across the genus, suggesting
412 that these could be examples of adaptive pleiotropy. Although we did not directly assess
413 the role of selection, our data indicate that the rapid floral trait evolution observed in this
414 group could have been facilitated by a relatively simple genetic basis for individual floral
415 traits, and a general absence of antagonistic pleiotropy among different types of

416 reproductive traits.

417

418 ***Few genetic changes could underlie floral trait shifts***

419 The relatively simple genetic architecture that we detect for most of our floral
420 traits might be one mechanism that has permitted rapid floral evolution within the genus.
421 Indeed, our inference that few QTL underlie corolla depth agrees with comparative
422 development data from these species (Kostyun *et al*., 2017) in which we observe that
423 relatively simple heterochronic changes in corolla trait growth rates distinguish these
424 rotate vs. tubular corolla forms. Interestingly, our findings are also consistent with
425 previous studies of floral trait genetics between closely related species (Smith, 2016), as
426 well as a quantitative genetics study of floral trait variation between two ecotypes of
427 *Jaltomata procumbens* (Mione & Anderson, 2017). In particular, Mione and Anderson
428 (2017) estimated 1-4 loci contributed to various floral traits, as well as petal spot
429 patterning. In other systems, one or few QTL have been found for species differences in
430 nectar volume (e.g. Bradshaw *et al*., 1998; Stuurman *et al*., 2004; Wessinger *et al*., 2014;
431 but see Nakazato *et al*., 2013), similar to our inference of a single QTL for this trait. For
432 petal and nectar color (including Lightness, color 'a' and color 'b'), we identified 4 and 7
433 QTL, respectively, with at least 1 QTL per trait with moderate or large effects (i.e. 10 -
434 33% PVE) (**Table 2; Table S6**), similar to other systems that generally identify few loci
435 of large effect for petal color (e.g. Bradshaw *et al*., 1998; Wessinger *et al*., 2014).
436 Perhaps unlike these cases, however, it is likely that loci controlling color differences in
437 *Jaltomata* are regulators of pigment quantity rather than presence/absence biosynthesis,
438 because both nectar and petal color show gradation in the BC1s rather than discrete color

439 bins. Based on synteny with domestic tomato, our identified petal color QTL occur on the
440 same chromosomes as several known anthocyanin biosynthesis genes (i.e. DFR on ch2,
441 CHS1 and F3H on ch9, and ANS1 on ch10, in tomato), but do not appear to overlap with
442 the chromosomal locations of these genes. Preliminary data from a VIGS (virus-induced
443 gene silencing) pilot study in *J. sinuosa* do indicate that the purple petal pigment is an
444 anthocyanin however (J.L. Kostyun and J.C. Preston, unpub.), whereas for nectar color,
445 preliminary data suggest that an indole-flavin contributes to red pigment in *J. umbellata*
446 (J.L. Kostyun and D. Haak, unpub.), consistent with our inference that color variation is
447 unassociated between these different floral components.

448 In addition to relatively few contributing loci, many of the examined floral traits
449 also appear to be underpinned by additive effects (**Table 1; Figure 2; Figures S3-S6**),
450 while epistatic effects were comparatively rare (see below). Both are factors that might
451 also facilitate more rapid responses to selection. Other studies have similarly found that
452 floral size traits are often additive (Gottlieb, 1984), including within *Jaltomata* (Mione &
453 Anderson, 2017). Although several floral traits showed transgressive segregation within
454 our BC1s, which could indicate epistatic interactions, similar patterns can result from
455 unique combinations of additive alleles that have opposite effects in the parental species
456 (e.g. deVicente & Tanksley, 1993) and we identified individual QTL with these opposing
457 effects for all traits with transgressive segregation (**Table S6; Figures S3-5**). In addition,
458 our models only detected significant interactions among QTL for ovary diameter and
459 nectar color 'a' (**Table S6**), consistent with a general lack of epistatic interactions for
460 floral traits. Therefore, while we may not have uncovered all epistatic interactions
461 contributing to our traits--because some QTL might be undetected in our study, and our

462 models did not assess between trait interactions--both QTL and overall segregation
463 patterns suggest that floral traits are primarily underpinned by additive rather than
464 epistatic effects.

465 In contrast, many of the fertility traits had segregation patterns consistent with
466 epistatic interactions. BC1 individuals tended to have lower seed set and poorer quality
467 seeds (decreased viability and response to germination-inducing stimuli), and the
468 recombinant BC population contained a subset of highly sterile individuals. The
469 segregation of recombinant individuals with reduced viability and fertility often occurs in
470 hybrids (Baack *et al*., 2015), including in hybrids from additional *Jaltomata* species pairs
471 (Kostyun & Moyle, 2017). Such patterns are typically due to deleterious epistatic
472 interactions between loci that have diverged between the two parental lineages, as has
473 been shown in close relatives including tomatoes (Moyle & Nakazato, 2008; Sherman *et*
474 *al*., 2014). These observations in *Jaltomata* are similarly consistent with a specific role
475 for epistasis among incompatible alleles in the expression of postzygotic reproductive
476 isolation.

477

478 ***Reduced constraints may also have facilitated rapid floral trait evolution***

479 Because rapid floral evolution may occur either through a lack of antagonistic
480 pleiotropy or through adaptive pleiotropy, we assessed evidence for these potential
481 mechanisms within *Jaltomata*. Within trait categories, we detected positive but modest
482 associations between several floral size traits, and among biologically related fertility
483 traits (e.g. fruit size and seed set) (**Figure 3; Table S3**), as well as significant co-
484 localization of QTL for these groups of traits (**Tables S7-S8**). Morphological associations

485 in particular suggest that shared growth regulators (e.g. Sicard & Lenhard, 2011; Brock *et*
486 *al*., 2012) contribute to observed variation in floral organ sizes, but do not completely
487 determine it; that is, overall floral size appears to share growth regulators (potentially
488 represented by co-localized QTL among floral size traits), but different floral organs also
489 appear to have unique growth regulator(s) (consistent with unique QTL). In contrast, we
490 detected fewer instances of strong trait correlations and QTL co-localization between
491 different trait categories (**Tables S3+S7-S8**). This general lack of antagonistic pleiotropy
492 among different classes of floral and fertility traits may have facilitated rapid floral
493 evolution in this system by minimizing constraints on the available combinations of floral
494 traits.

495 Despite this general pattern, we did identify several instances of QTL co-
496 localization that might represent adaptive pleiotropy, specifically among different corolla
497 and nectar traits. Overall, these associations would have produced flowers with larger
498 corolla limbs, deeper corolla tubes, and a greater volume of darker colored nectar (**Table**
499 **2; Figure 4; Tables S6+S8**). Interestingly, this trait combination (large flowers with
500 copious dark nectar) is actually not exhibited by either parental species used in this
501 experiment (**Figure 1; Table 1**); however, it is found in numerous other *Jaltomata*
502 species and is consistent with suspected pollination syndromes within the genus (see
503 below; Miller *et al*., 2011; Kostyun & Moyle, 2017). Correlated changes in corolla size
504 and nectar volume have also been observed in several other systems, including those with
505 documented or hypothesized pollinator shifts (e.g. *Petunia*, *Mimulus*, and *Penstemon*;
506 Galliot et al. 2006; reviewed in Smith, 2016).
507

508 ***Ecological context for rapid floral change in* Jaltomata**

509 Overall, our findings suggest potential mechanistic explanations for the evolution
510 of remarkable floral trait diversity among *Jaltomata* species within the last 5 million
511 years (Sarkinen *et al*., 2013). Traits with a relatively simple genetic basis that are
512 uncoupled from other floral and fertility traits have fewer mechanistic constraints, and
513 therefore can more rapidly respond to selective opportunities as they arise (given
514 sufficient standing or new genetic variation) (Agrawal & Stinchcombe, 2009; Smith,
515 2016). Although we have not yet directly assessed the role of selection in shaping floral
516 differences among species, several features of *Jaltomata* floral biology are consistent
517 with pollinator-mediated selection on floral traits (van der Niet & Johnson, 2012), likely
518 in conjunction with mating-system related changes (Goodwillie *et al*., 2010). First, floral
519 trait variation within *Jaltomata* shows clear hallmarks of selection imposed by pollinator
520 differentiation. Of the two main lineages within the genus, nearly all species in the
521 Central and South American clade have relatively small, ancestrally rotate flowers with
522 small amounts of lightly colored nectar (Wu et al. 2018), and hymenopterans have been
523 observed visiting several of these species in their native range (T. Mione, pers. comm.).
524 In contrast, many species in the clade that is restricted to South America—including *J.*
525 *umbellata* examined here—have floral features associated with attraction of vertebrate
526 pollinators (Fenster *et al*., 2004). Several of these species with larger flowers, a highly
527 fused corolla (either campanulate or tubular), and copious amounts of darkly colored
528 nectar are visited by hummingbirds (T. Mione, per. comm.); intriguingly, this repeated
529 natural trait covariation is consistent with the genetic association between floral size and
530 nectar traits we identified here.

531 These features indicate that shifts among different types of pollinators are a likely
532 source of selection for floral differentiation among species within *Jaltomata*, however,
533 mating system variation in the genus may also have facilitated these transitions. Self-
534 incompatibility is the ancestral state in the Solanaceae (Steinbachs & Holsinger, 2002)
535 and is broadly persistent in close relatives *Solanum* and *Capsicum* (Goldberg *et al*.,
536 2010). In contrast, all examined *Jaltomata* species are self-compatible (Mione, 1992;
537 Kostyun & Moyle, 2017; J.L. Kostyun & T. Mione, unpub.), indicating that gametophytic
538 self-incompatibility was lost early in the evolution of this clade. The presence of delayed
539 selfing and strong herkogamy in many species (e.g. Mione *et al*., 2015; Mione *et al*.,
540 2019), in addition to field observations of pollinators (above; T. Mione, pers. comm.),
541 indicate that species most likely employ a mixed mating strategy in their native ranges.
542 Mixed mating strategies are generally observed to maintain the largest amount of floral
543 trait variation, compared to predominant selfing or enforced outcrossing (Goodwillie *et*
544 *al*., 2005; Rosas-Guerrero *et al.,* 2014). In addition, they have been predicted to facilitate
545 pollinator shifts--especially to pollinators that might be more efficient but potentially
546 unreliable (such as hummingbirds)—because they allow reproductive assurance (via
547 selfing, when pollinators are limited) and increase the expression of new floral trait
548 variation controlled by recessive alleles (Goodwillie *et al*., 2005; Brys *et al*., 2013;
549 Wessinger & Kelly, 2018). Notably, our data indicate that dark/red colored nectar is at
550 least partially recessive (**Figure 2**), and that red petal pigmentation is completely
551 recessive (**Figure S7**), consistent with this novel variation being based on new recessive
552 alleles. Together, these observations are intriguing as they suggest that mixed mating, in
553 conjunction with the specific genetic architecture of floral trait variation, might have

554 facilitated the evolution of new floral trait variation in *Jaltomata*.

555

556 **CONCLUSIONS**

557 Genetic correlations among floral traits, especially those due to pleiotropic
558 effects, likely shape permitted trajectories of floral evolution. To assess how such genetic
559 associations might have contributed to observed patterns of floral diversity in *Jaltomata*,
560 we examined segregation patterns and genetic architecture of 25 floral and fertility traits
561 in a hybrid (BC1) population generated from parents with divergent floral traits. Our data
562 are consistent with several mechanisms that could have allowed rapid floral trait
563 evolution in this system: a largely simple genetic basis underlying variation in most of
564 our floral traits, a general absence of antagonistic pleiotropy constraining floral evolution,
565 and a potential instance of adaptive pleiotropy governing floral size and nectar traits. This
566 genetic architecture, in combination with pollinator-mediated selection on a background
567 of self-compatible mixed mating, might have uniquely positioned this genus for the rapid
568 floral diversification now evident within *Jaltomata*.

569

570 **ACKNOWLEDGEMENTS**

571 We thank the IU greenhouse staff for plant care, CJ Jewell and David Haak for
572 logistical support, undergraduate research assistants (especially Meret Thomas-Huebner,
573 Devki Shukla, and Shachia Jackson) for assistance with data collection, Tim Leslie for
574 assistance with simulations, and Mark Rausher and two anonymous reviewers for
575 feedback on a previous version of the manuscript. This work was supported by the IU
576 Biology Department, National Science Foundation Award (NSF DEB 1136707) to LCM,

and National Science Foundation Graduate Research Fellowship Program (NSF DEB 1342962) and Doctoral Dissertation Improvement Grant (NSF DEB 1601078) to JLK.

AUTHOR CONTRIBUTIONS

JLK and LCM designed the experiment, JLK generated experimental materials, JLK and CMK collected phenotypic data, JLK and MJSG analyzed the data, and JLK and LCM wrote the paper with input from CMK and MJSG.

REFERENCES

Agrawal AF, Stinchcombe JR. 2009. How much do genetic covariances alter the rate of adaptation? *Proc R Soc Lond Biol* **276**:1183-1191.

Andrews S. 2010. FastQC: a quality control tool for high throughput sequence data. Available online at: http://www.bioinformatics.babraham.ac.uk/projects/fastqc

Armbruster WS, Hansen TF, Pelabon C, Perez-Barrales R, Maad J. 2009. The adaptive accuracy of flowers: measurement and microevolutionary patterns. *Ann Bot* **103**:1529-1545.

Armbruster WS, Pelabon C, Bolstad GH, Hansen TF. 2014. Integrated phenotypes: understanding trait covariation in plants and animals. *Proc R Soc Lond Biol* **369**.

Baack E, Melo MC, Rieseberg LH, Ortiz-Barrientos D. 2015. The origins of reproductive isolation in plants. *New Phytol* **207**:968-984.

Bartlett ME. 2017. Changing MADS-Box Transcription Factor Protein–Protein Interactions as a Mechanism for Generating Floral Morphological Diversity. *Integrative and Comparative Biology* **57**:1312-1321.

600 **Bradshaw HD, Otto KG, Frewen BE, McKay JK, Schemske DW. 1998**. Quantitative
601 trait loci affecting differences in floral morphology between two species of
602 monkeyflower (*Mimulus*). *Genetics* **149**:367-382.
603 **Brock MT, Kover PX, Weinig C. 2012**. Natural variation in GA1 associates with floral
604 morphology in *Arabidopsis thaliana*. *New Phytol* **195**:58-70.
605 **Broman KW**. 2001. Review of statistical methods for QTL mapping in experimental
606 crosses. *Lab Animal (NY)* **30**:44-52.
607 **Broman KW, Wu H, Sen S, Churchill GA. 2003**. R/qtl: QTL mapping in experimental
608 crosses. *Bioinformatics* 19:889-890.
609 **Brys R, Geens B, Beeckman T, Jacquemyn H. 2013**. Differences in dichogamy and
610 herkogamy contribute to higher selfing in contrasting environments in the annual
611 *Blackstonia perfoliata* (Gentianaceae). *Ann Bot* **111**:651-661.
612 **Bolger AM, Lohse M, Usadel B. 2014**. Trimmomatic: A flexible trimmer for Illumina
613 Sequence Data. *Bioinformatics*, btu170.
614 **Catchen J, Hohenlohe PA, Bassham S, Amores A, Cresko WA. 2013**. Stacks: an
615 analysis tool set for population genomics. *Mol Ecol* 22: 3124-3140.
616 **Chiarini FE, Lipari D, Barboza GE, Knapp S. 2017**. IAPT/IOPB chromosome data
617 25. *Taxon* 66: 1246–1252.
618 **Conner JK. 2002**. Genetic mechanisms of floral trait correlations in a natural population.
619 *Nature* **420**:407-410.
620 **Conner JK, Cooper IA, La Rosa RJ, Perez SG, Royer AM. 2014**. Patterns of
621 phenotypic correlations among morphological traits across plants and animals.
622 *Phil. Trans. R. Soc. B* **369**.

623 **deVicente MC, Tanksley SD. 1993**. QTL analysis of transgressive segregation in an
624 interspecific tomato cross. *Genetics* **134**:585-596.
625 **Ettensohn CA. 2013**. Encoding anatomy: Developmental gene regulatory networks and
626 morphogenesis. *Genesis* **51**:383-409.
627 **Farooq M, Basra SMA, Ahmad N, Hafeez K. 2005**. Thermal hardening: A new seed
628 vigor enhancement tool in rice. *J Integr Plant Biol* **47**:187-193.
629 **Fenster CB, Armbruster WS, Wilson P, Dudash MR, Thomson JD. 2004**. Pollination
630 syndromes and floral specialization. *Annu Rev Ecol Evol Syst* **35**:375-403.
631 **Galliot C, Hoballah ME, Kuhlemeier C, Stuurman J. 2006.** Genetics of flower size
632 and nectar volume in *Petunia* pollination syndromes. *Planta* **225**:203-212.
633 **Garcia JE, Greentree AD, Shrestha M, Dorin A, Dyer AG. 2014**. Flower Colours
634 through the Lens: Quantitative Measurement with Visible and Ultraviolet Digital
635 Photography. *Plos One* **9**.
636 **Goldberg EE, Kohn JR, Lande R, K. Robertson KA, Smith SA, Igic B. 2010**. Species
637 selection maintains self-incompatibility. *Science* **330**:493-495.
638 **Goodwillie C, Kalisz S, Eckert CG. 2005**. The evolutionary enigma of mixed mating
639 systems in plants: Occurrence, theoretical explanations, and empirical evidence.
640 *Annu Rev Ecol Evol Syst* **36**:47-79.
641 **Goodwillie C, Sargent RD, Eckert CG, Elle E, Geber MA, Johnston MO, Kalisz S,**
642 **Moeller DA, Ree RH, Vallejo-Marin M et al. 2010.** Correlated evolution of
643 mating system and floral display traits in flowering plants and its implications for
644 the distribution of mating system variation. *New Phytol* **185**:311-321.
645 **Gottlieb LD. 1984**. Genetics and morphological evolution in plants. *Am Nat* **123**:681-

646 709.

647 **Hermann K, Klahre U, Moser M, Sheehan H, Mandel T, Kuhlemeier C. 2013**. Tight
648 Genetic Linkage of Prezygotic Barrier Loci Creates a Multifunctional Speciation
649 Island in *Petunia*. *Current Biology* **23**:873-877.

650 **Jewell C, Papineau AD, Freyre R, Moyle LC. 2012**. Patterns of reproductive isolation
651 in *Nolana* (chilean bellflower). *Evolution* **66**:2628-2636.

652 **Kendal D, Hauser CE, Garrard GE, Jellinek S, Giljohann KM, Moore JL. 2013**.
653 Quantifying Plant Colour and Colour Difference as Perceived by Humans Using
654 Digital Images. *Plos One* **8**.

655 **Knapp S. 2010**. On 'various contrivances': pollination, phylogeny and flower form in the
656 Solanaceae. *Phil Trans R Soc B* **365**:449-460.

657 **Kostyun JL, Moyle LC. 2017**. Multiple strong postmating and intrinsic postzygotic
658 reproductive barriers isolate florally diverse species of *Jaltomata* (Solanaceae).
659 *Evolution* **71**:1556-1571.

660 **Kostyun JL, Preston JC, Moyle LC. 2017**. Heterochronic developmental shifts underlie
661 floral diversity within *Jaltomata* (Solanaceae). *EvoDevo* **8**:17.

662 **Li H. 2013**. Aligning sequence reads, clone sequences and assembly contigs with BWA-
663 MEM. arXiv:1303.3997v1 [q-bio.GN].

664 **Manceau M, Domingues VS, Mallarino R, Hoekstra HE. 2011**. The Developmental
665 Role of Agouti in Color Pattern Evolution. *Science* **331**:1062-1065.

666 **Miller RJ, Mione T, Phan HL, Olmstead RG. 2011**. Color by Numbers: Nuclear Gene
667 Phylogeny of *Jaltomata* (Solanaceae), Sister Genus to *Solanum*, Supports Three
668 Clades Differing in Fruit Color. *Syst Botany* **36**:153-162.

Mione T. 1992. *The systematics and evolution of* Jaltomata *(Solanaceae)*. PhD Dissertation, The University of Connecticut. Available from ProQuest Dissertations & Theses Global. (303964972).

Mione T, Anderson GJ. **2017.** Genetics of floral traits of *Jaltomata procumbens* (Solanaceae). *Brittonia* **69**:1-10.

Mione T, Anderson GJ, Nee M. 1993. *Jaltomata* I: Circumscription, description and new combinations for five South American species. *Brittonia* **45**: 138-145.

Mione T, Leiva González S, Yacher L. 2015. Two new Peruvian species of *Jaltomata* (Solanaceae, Solaneae) with red floral nectar. *Brittonia* **67**:105-112.

Mione T, Plourd KC, Leiva González S, Yacher L, Philbrick CT, Blume D. 2017. Pollination decreases longevity of the protogynous flowers of *Jaltomata sinuosa* (Solanaceae). *J Biol Nat* **7**:123-129.

Mione T, Kostyun JL, Leiva González S. 2019. Breeding system features and a novel method for locating the floral nectar secretion in a South American nightshade (*Jaltomata quipuscoae*, Solanaceae). *Plant Biosystems* March:1-10. https://doi.org/10.1080/11263504.2019.1578277.

Moyle LC, Nakazato T. 2008. Comparative genetics of hybrid incompatibility: Sterility in two *Solanum* species crosses. *Genetics* **179**:1437-1453.

Nakazato T, Rieseberg LH, Wood TE. 2013. The genetic basis of speciation in the Giliopsis lineage of *Ipomopsis* (Polemoniaceae). *Heredity* **111**:227-237.

Olmstead RG, Bohs L, Migid HA, Santiago-Valentin E, Garcia VF, Collier SM. 2008. A molecular phylogeny of the Solanaceae. *Taxon* **57**:1159-1181.

Preston JC, Hileman LC, Cubas P. 2011. Reduce, reuse, and recycle: developmental

692 evolution of trait diversification. *Am. J. Bot.* **98**:397-403.

693 **RAW Therapee Team. 2012**. Raw Therapee: cross-platform raw image processing

694 program. http://rawtherapee.com/.

695 **Rijpkema A, Gerats T, Vandenbussche M. 2006**. Genetics of floral development in

696 Petunia. In Soltis DE, Soltis PS, Callow JA, eds. *Adv Bot Res: Developmental*

697 *Genetics of the Flower.* Elsevier Ltd, 237-278.

698 **Rosas-Guerrero V, Aguilar T, Marten-Rodriguez S, Ashworth L, Lopezaraiza-**

699 **Mikel M, Bastida JM, Quesada M. 2014**. A quantitative review of pollination

700 syndromes: do floral traits predict effective pollinators? *Ecol. Lett* **17**:388-400.

701 **Sarkinen T, Bohs L, Olmstead RG, Knapp S. 2013**. A phylogenetic framework for

702 evolutionary study of the nightshades (Solanaceae): a dated 1000-tip tree. *BMC*

703 *Evolutionary Biology* **13**.

704 **Schneider CA, Rasband WS, Eliceiri KW. 2012**. NIH Image to ImageJ: 25 years of

705 image analysis. *Nature Methods* **9**:671-675.

706 **Schwartzwald D. 2012**. Color Space Converter Plugin for ImageJ.

707 https://imagej.nih.gov/ij/plugins/color-space-converter.html.

708 **Sherman NA, Victorine A, Wang RJ, Moyle LC. 2014**. Interspecific Tests of Allelism

709 Reveal the Evolutionary Timing and Pattern of Accumulation of Reproductive

710 Isolation Mutations. *Plos Genetics* **10**.

711 **Shrestha R, Gomez-Ariza J, Brambilla V, Fornara F. 2014**. Molecular control of

712 seasonal flowering in rice, arabidopsis and temperate cereals. *Ann Bot* **114**:1445-

713 1458.

714 **Sicard A, Lenhard M. 2011**. The selfing syndrome: a model for studying the genetic

715 and evolutionary basis of morphological adaptation in plants. *Ann Bot* **107**:1433-
716 1443.
717 **Smaczniak C, Immink RGH, Angenent GC, Kaufmann K. 2012**. Developmental and
718 evolutionary diversity of plant MADS-domain factors: insights from recent
719 studies. *Development* **139**:3081-3098.
720 **Smith SD. 2016**. Pleiotropy and the evolution of floral integration. *New Phytol* **209**:80-
721 85.
722 **Stebbins GL. 1974**. Flowering plants: evolution above the species level. Harvard
723 University Press, Cambridge, MA.
724 **Steinbachs JE, Holsinger KE. 2002**. S-RNase-mediated gametophytic self
725 incompatibility is ancestral in eudicots. *Mol Biol Evol* **19**: 825–829.
726 **Stuurman J, Hoballah ME, Broger L, Moore J, Basten C, Kuhlemeier C. 2004**.
727 Dissection of floral pollination syndromes in *Petunia*. *Genetics* **168**:1585-1599.
728 **Taylor J, Butler D. 2017**. R Package ASMap: Efficient Genetic Linkage Map
729 Construction and Diagnosis. *Journal of Statistical Software* **79**:1-29.
730 **Tomato Genome Consortium, The. 2012**. The tomato genome sequence provides
731 insights into fleshy fruit evolution. *Nature* **485**:635-641.
732 **van der Niet T, Johnson SD. 2012**. Phylogenetic evidence for pollinator-driven
733 diversification of angiosperms. *Trends Ecol Evolut* **27**:353-361.
734 **Wagner GP, Zhang JZ. 2011**. The pleiotropic structure of the genotype-phenotype map:
735 the evolvability of complex organisms. *Nature Reviews Genetics* **12**:204-213.
736 **Wessinger CA, Hileman LC, Rausher MD. 2014**. Identification of major quantitative
737 trait loci underlying floral pollination syndrome divergence in *Penstemon*. *Phil.*

Trans. R. Soc. B **369**.

Wessinger CA, Freeman CC, Mort ME, Rausher MD, Hileman LC. 2016. Multiplexed shotgun genotyping resolves species relationships within the North American genus *Penstemon*. *Am J Bot* **103**:912-922.

Wessinger CA, Kelly JK. 2018. Selfing can facilitate transitions between pollination syndromes. *Am Nat* **191**.

Wu M, Kostyun JL, Hahn MW, Moyle LC. 2018. Dissecting the basis of novel trait evolution in a radiation with widespread phylogenetic discordance. *Mol Ecol* **27**: 3301-3316.

Wu M, Kostyun JL, Moyle LC. 2019. Genome sequence of *Jaltomata* addresses rapid reproductive trait evolution and enhances comparative genomics in the hyper-diverse Solanaceae. *Genome Biology and Evolution* in press. Available at: https://www.biorxiv.org/content/early/2018/05/30/335117.

Xu SQ, Schluter PM. 2015. Modeling the two-locus architecture of divergent pollinator adaptation: how variation in SAD paralogs affects fitness and evolutionary divergence in sexually deceptive orchids. *Ecology and Evolution* **5**:493-502.

Table 1. Summary statistics for floral and fertility traits in parental species, F1s, and BC1s. Phenotypic means and variances provided, while significant differences between parental species were assessed with t-tests on transformed data as appropriate (see Methods). Note that differences in seed germination rates were not tested. * p<0.05, ** p<0.001; *** p<0.0001.

Trait	*J. sinuosa* (n=7)		*J. umbellata* (n=5)	
Floral Morphology	**Mean**	**Variance**	**Mean**	**Variance**
Buds per Inflorescence	*2.86***	0.03	8.60	3.24
Calyx Diameter (mm)	*15.49***	0.08	8.14	2.91
Sepal Length (mm)	*7.48***	0.02	4.41	0.56
Corolla Diameter (mm)	*29.82****	1.92	15.32	5.70
Corolla Depth (mm)	*1.38***	0.07	10.25	5.52
Corolla Fusion (mm)	9.45	0.11	10.33	1.55
Corolla Fusion Proportion	*0.63**	0.001	0.72	0.001
Petal Length (mm)	14.85	0.41	14.40	0.16
Stamen Length (mm)	10.80	0.29	10.45	0.22
Anther Length (mm)	*2.03**	0.02	1.73	0.04
Ovary Diameter (mm)	*2.28****	0.03	1.37	0.05
Style Length (mm)	*7.90****	0.17	14.64	1.72
Herkogamy (mm)	*-2.20****	0.01	5.37	4.62
Floral Color + Physiology				
Nectar Color - L	*83.49****	20.32	*50.42****	31.63
Nectar Color - a	*-1.55****	0.95	*57.61****	7.10
Nectar Color - b	*3.47****	8.20	*71.84****	59.31
Petal Color - L	83.18	2.59	84.15	4.86
Petal Color - a	*0.81**	0.02	*-0.93**	0.62
Petal Color -b	*-1.26****	0.02	*6.71****	1.05
Nectar Volume (uL)	*6.86****	1.07	17.80	13.20
Fertility				
Viable Pollen Grains	25000	36800000	27000	60770000
Proportion Viable Pollen	0.76	0.01	0.71	0.02
Fruit Set	*0.93**	0.01	0.55	0.06
Fruit Mass (g)	*0.47***	0.01	0.12	0.01
Fruit Diameter (cm)	*1.01**	0.01	0.61	0.02
Seed Set	*74.87**	256.92	30.44	494.43
Viable Seed Set	*74.87**	256.92	23.59	182.31
Viable Seed T50	9.33	--	7.00	--
Viable Seed MGT	22.00	--	14.00	--

Table 1 cont.

F1s (n=13)		BC1s (n=224)	
Mean	**Variance**	**Mean**	**Variance**
3.95	0.68	3.51	1.63
10.55	0.48	12.10	1.08
5.45	0.13	6.16	0.28
24.58	6.84	28.97	9.92
6.64	0.58	5.22	1.35
9.81	0.40	9.92	1.24
0.67	0.001	0.63	0.002
14.65	1.61	15.78	2.88
10.81	0.59	10.86	1.26
2.01	0.01	2.13	0.04
1.62	0.02	1.82	0.04
12.39	1.04	10.82	1.97
2.95	1.08	1.20	1.02
81.31	14.35	83.99	13.42
-0.05	101.74	-4.29	14.91
59.85	75.94	22.91	287.97
86.93	5.82	83.56	4.60
-0.81	0.19	-0.04	0.36
2.89	3.13	0.75	1.29
11.90	12.32	10.76	18.87
22513	16602405	26886	145318716
0.82	0.00	0.74	0.03
0.93	0.01	0.89	0.03
0.24	0.01	0.29	0.01
0.80	0.01	0.85	0.03
36.06	168.37	37.67	361.12
25.46	303.95	26.28	340.08
34.00	1001.78	26.70	607.37
46.04	622.37	39.36	458.11

Table 2. QTL for key floral and fertility traits. Includes peak location and LOD of each QTL, 1.5 LOD intervals, proportion phenotypic variance explained, phenotypic effect size and standard error, proportion of parental trait difference explained, and whether the effect is aligned with parental trait values. Comprehensive QTL data, including the full models for all traits, are provided in Table S6. Note: effect sizes are given as the difference between homozygote and heterozygote mean phenotypes (i.e. the effect of a single paternal allele at that QTL), while the proportion of parental trait difference corresponds to the relative homozygous effect (RHE).

Trait	Linkage Group	Peak Location (1.5 LOD Interval)	Peak LOD
Flower Morphology			
Calyx Diameter (3)	1	56 (49-81)	9.06
	8	84.3 (69-92.55)	3.15
	9	66 (17-85)	5.59
Corolla Diameter (3)	4	21.1 (13-70)	3.50
	8	73.1 (67-84)	5.87
	12	37.4 (0-65.17)	1.57
Corolla Depth (4)	5	40.8 (20-46)	10.19
	7	52 (48-60.67)	17.95
	9	30 (11-38)	12.38
	10	55.8 (41-91)	4.48
Corolla Fusion Prop. (4)	1	72 (57-106)	4.60
	4	26 (19-84)	3.77
	5	86 (80.21-99)	3.57
	9	16 (0-67)	7.19
Petal Length (3)	7	100 (25-100.67)	2.46
	8	73 (39-92.55)	3.55
	12	48.2 (0-65.17)	2.04
Stamen Length (4)	2	37.5 (6-61)	4.54
	4	120.8 (100-133)	3.77
	7	91 (59-100.67)	4.45
	9	0 (0-33)	5.32
Anther Length (1)	1	18 (8-35.87)	3.78

Table 2. cont.

Ovary Diameter (4)	1	68 (60-107)	5.77
	5	72 (0-84)	2.53
	7	9.9 (0-25)	3.56
	12	48.2 (5-65.17)	4.31
Style Length (2)	2	95.2 (55-126)	2.79
	9	22 (1-30)	9.89
Flower Physiology			
Nectar Volume (1)	3	187.2 (172-187.19)	2.81
Flower Color			
Nectar L (2)	2	154.9 (147-171.87)	2.97
	5	103.9 (74-115.35)	6.44
Nectar a (4)	3	66.1 (60-95)	7.69
	4	14 (0-23.74)	3.99
	7	29.1 (10-42)	2.32
	7	56.2 (43-63)	3.54
Nectar b (4)	2	152 (141-171.87)	4.50
	3	186 (164-187.19)	2.83
	5	100 (94-111)	11.00
	7	26 (20.02-32)	9.02
Petal L (2)	4	23.7 (0-81)	2.40
	5	65.3 (58-71)	3.83
Petal a (4)	5	62 (58-68)	12.11
	8	52 (49-52.48)	8.54
	8	52.5 (52-53)	8.13
	9	64.1 (44-76)	9.89
Petal b (3)	5	64 (60-69)	21.46
	9	52 (52-54)	5.60
	9	55.8 (54.05-57)	4.22
Fertility			
Fruit Diameter (2)	1	80 (61-103)	4.67
	11	76.9 (51-79.93)	3.09
Fruit Mass (4)	1	96 (60-146)	5.95
	3	170 (48-187.19)	2.99
	11	76.5 (54-79.93)	4.19
	12	0 (0-10.64)	4.66
Seed Set (2)	11	76 (63-79.93)	6.64
	12	0 (0-63)	2.86
Viable Seed Set (1)	11	76.9 (68-79.93)	4.42

789 **Table 2. cont.**

%PVE	Effect ± SE	%Parental Trait Difference (RHE)	Aligned with Parental Value?
13.67	-0.803 ± 0.120	0.22	Y
4.46	-0.457 ± 0.120	0.12	Y
8.13	-0.598 ± 0.116	0.16	Y
4.47	1.387 ± 0.344	-0.19	N
7.69	-1.902 ± 0.360	0.26	Y
1.96	-0.963 ± 0.361	0.13	Y
11.20	0.844 ± 0.119	0.19	Y
21.47	1.146 ± 0.116	0.26	Y
13.94	0.942 ± 0.119	0.21	Y
4.64	-0.521 ± 0.114	-0.12	N
7.02	-0.022 ± 0.005	-0.56	N
5.70	-0.021 ± 0.005	-0.53	N
5.39	0.022 ± 0.005	0.56	Y
11.27	0.029 ± 0.005	0.74	Y
3.29	0.018 ± 0.005	-2.66	N
4.78	-0.022 ± 0.005	3.32	Y
2.71	-0.017 ± 0.005	2.50	Y
5.80	-0.548 ± 0.119	3.18	Y
4.78	-0.499 ± 0.119	2.90	Y
5.68	0.551 ± 0.121	-3.20	N
6.86	0.619 ± 0.124	-3.60	N
6.48	-0.116 ± 0.027	0.78	Y

790

791

792

793

794

795

796

797

Table 2. cont.

9.21	-0.120 ± 0.023	0.26	Y
3.90	0.092 ± 0.027	-0.20	N
5.56	-0.094 ± 0.023	0.21	Y
6.78	-0.104 ± 0.023	0.23	Y
3.80	0.022 ± 0.006	0.16	Y
14.51	0.044 ± 0.006	0.33	Y
5.22	0.098 ± 0.027	0.48	Y
5.12	-0.008 ± 0.002	0.08	Y
11.51	-0.014 ± 0.003	0.13	Y
13.04	0.062 ± 0.010	0.23	Y
6.51	-0.043 ± 0.010	-0.16	N
3.72	-0.040 ± 0.012	-0.15	N
5.74	0.050 ± 0.012	0.18	Y
5.25	0.161 ± 0.036	0.27	Y
3.24	0.138 ± 0.038	0.23	Y
13.74	0.288 ± 0.039	0.48	Y
11.03	0.230 ± 0.035	0.39	Y
4.43	0.005 ± 0.002	2.03	Y
7.19	0.007 ± 0.002	2.92	Y
15.28	-0.122 ± 0.016	0.44	Y
10.35	-1.355 ± 0.210	4.81	Y
9.82	1.312 ± 0.209	-4.65	N
12.18	-0.097 ± 0.014	0.35	Y
32.83	0.210 ± 0.019	0.56	Y
7.20	0.486 ± 0.094	1.31	Y
5.35	-0.415 ± 0.093	-1.11	N
8.64	-0.026 ± 0.005	0.52	Y
5.61	-0.020 ± 0.005	0.40	Y
9.35	-0.026 ± 0.005	0.44	Y
4.56	-0.018 ± 0.002	0.31	Y
6.46	-0.021 ± 0.005	0.35	Y
7.22	-0.023 ± 0.005	0.40	Y
12.28	-0.157 ± 0.028	0.65	Y
5.07	-0.109 ± 0.030	0.45	Y
8.85	-0.211 ± 0.046	0.75	Y

801 **Figure Legends.**

802 **Figure 1**. Representative flowers of the parental species and their F1 hybrid.

803

804 **Figure 2**. Key trait distributions within the BC1 population, compared to phenotypic

805 means for *J. sinuosa* (purple line), *J. umbellata* (red line), and their F1s (pink line).

806

807 **Figure 3**. Key floral trait correlations within the BC1 mapping population. Scatterplots

808 are provided below the diagonal, while Spearman's correlation coefficients and

809 associated p-values are above the diagonal. Statistically significant correlations following

810 Bonferroni correction ($p < 5.945 \times 10^{-5}$) are highlighted in red. Correlation values for all

811 traits are provided in Table S3, and for PC traits provided in Table S5.

812

813 **Figure 4**. Linkage map and distribution of identified QTL (including 1.5 LOD intervals)

814 for 12 key floral and fertility traits.

815

816

817 **Supplementary Information**

818 **Table S1.** Accession information for material used and generated in this study.

819 **Table S2**. Trait measurements for all individuals phenotyped.

820 **Table S3**. Correlations among all measured traits within BC1 individuals.

821 **Table S4**. Principal component loadings for highly correlated traits.

822 **Table S5**. Correlations among PC traits within BC1 individuals

823 **Table S6**. Full QTL models for all examined traits.

824 **Table S7**. Expected and observed counts of QTL overlap.

825 **Table S8**. Identified instances of QTL co-localization, based on overlapping 1.5 LOD

826 intervals.

827 **Figure S1**. Measured morphological traits on mature flowers.

828 **Figure S2**: Biplots following PCA on floral morphological traits

829 **Figures S3-S4**: Distributions for floral morphological traits within the mapping

830 population.

831 **Figure S5**. Distributions for physiological and color traits within the mapping population.

832 **Figure S6**. Distributions for fertility traits within the mapping population.

833 **Figure S7**. Representative examples of petal and nectar color variation among F1

834 individuals, compared to either parent.

835 **Figure S8**. Comparison of observed number of QTL overlaps with counts from 10000

836 randomly generated simulations, for QTL co-localization overlap within and between

837 trait categories (morphology, color, and fertility).

838

839

840

841

842

843

J. sinuosa
F1
J. umbellata
1 cm

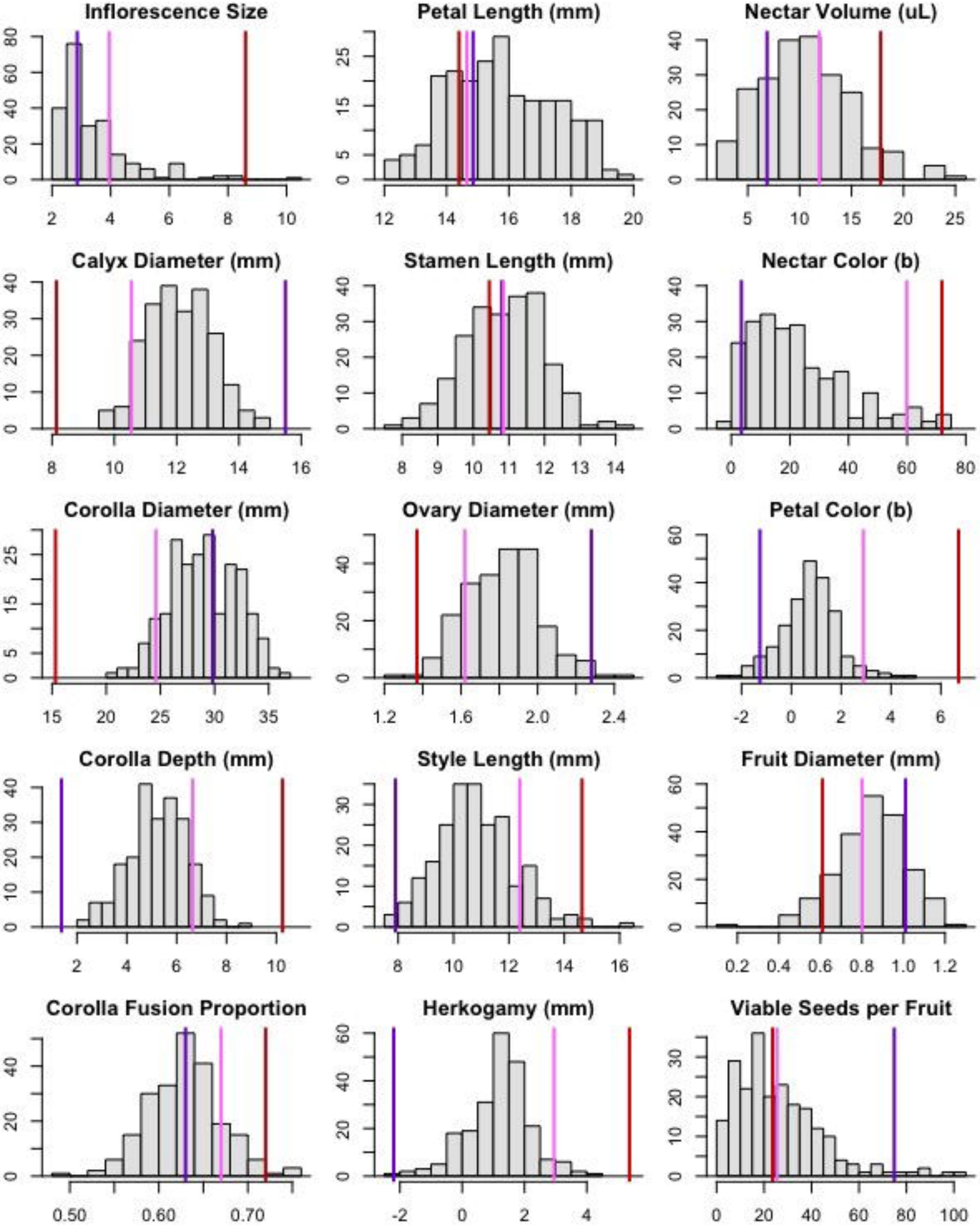
Inflorescence Size
Petal Length (mm)
Nectar Volume (uL)
Calyx Diameter (mm)
Stamen Length (mm)
Nectar Color (b)
Corolla Diameter (mm)
Ovary Diameter (mm)
Petal Color (b)
Corolla Depth (mm)
Style Length (mm)
Fruit Diameter (mm)
Corolla Fusion Proportion
Herkogamy (mm)
Viable Seeds per Fruit

Calyx Dia	r=0.656 p<1.02e-6	r=0.052 p=0.440	r=-0.162 p=0.015	r=0.105 p=0.118	r=0.571 p<1.02e-6	r=0.001 p=0.989	r=0.176 p=0.008	r=-0.001 p=0.986	r=-0.145 p=0.030
	Cor Dia	r=0.216 p=0.001	r=-0.348 p<1.02e-6	r=0.380 p<1.02e-6	r=0.448 p<1.02e-6	r=0.455 p<1.02e-6	r=0.286 p=1.33e-5	r=0.307 p=2.88e-5	r=-0.268 p=4.94e-5
		Cor Depth	r=0.208 p=0.002	r=0.122 p=0.067	r=0.198 p=0.003	r=0.277 p=2.68e-5	r=0.142 p=0.033	r=0.169 p=0.011	r=0.113 p=0.092
			Cor Fus Prop	r=0.088 p=0.191	r=-0.076 p=0.257	r=-0.026 p=0.665	r=-0.070 p=0.295	r=-0.121 p=0.071	r=0.222 p=0.0008
				Stam Length	r=0.015 p=0.827	r=0.511 p<1.02e-6	r=0.098 p=0.144	r=0.204 p=0.0022	r=-0.040 p=0.550
					Ovary Dia	r=-0.056 p=0.406	r=0.267 p=0.0001	r=0.001 p=0.988	r=0.015 p=0.823
						Style Length	r=0.159 p=0.018	r=0.372 p<1.02e-6	r=-0.065 p=0.336
							Nec Vol	r=0.189 p=0.0046	r=-0.032 p=0.336
								Nec Color (b)	r=0.06 p=0.369
									Pet Color (b)

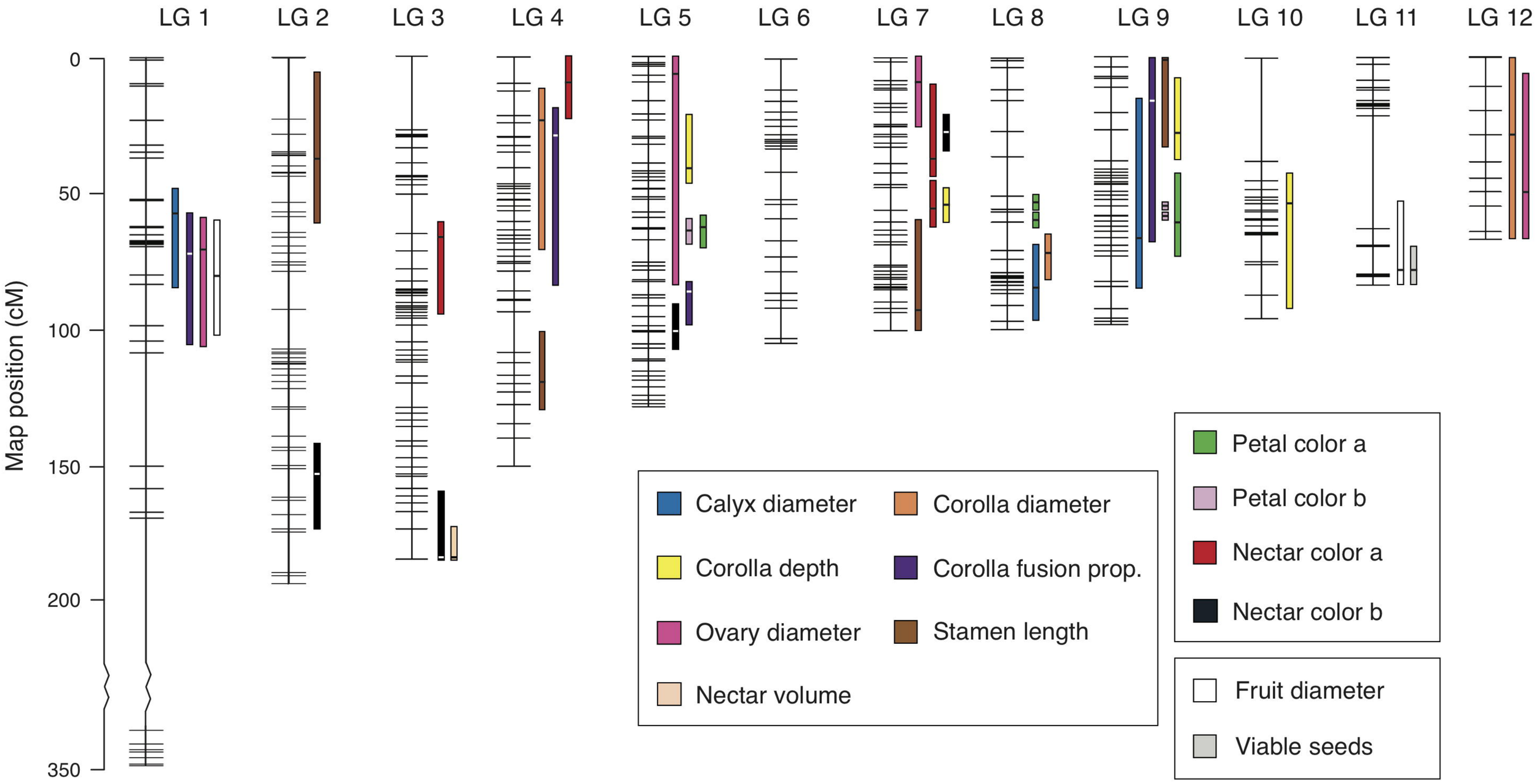
LG 1
LG 2
LG 3
LG 4
LG 5
LG 6
LG 7
LG 8
LG 9
LG 10
LG 11
LG 12
Map position (cM)
0
50
100
150
200
350
Calyx diameter
Corolla diameter
Corolla depth
Corolla fusion prop.
Ovary diameter
Stamen length
Nectar volume
Petal color a
Petal color b
Nectar color a
Nectar color b
Fruit diameter
Viable seeds